



**AFRL-RH-FS-TR-2016-0018**

**The Effects of Scattered Light from Optical  
Components on Visual Function**

Thomas K. Kuyk  
Peter A. Smith  
Solangia N. Engler  
Paul V. Garcia  
William R. Brockmeier  
**Engility Corporation**

Brenda A. Novar  
Christopher M. Putnam  
Leon N. McLin  
**711th Human Performance Wing  
Airman Systems Directorate  
Bioeffects Division  
Optical Radiation Bioeffects Branch**

**February 2016  
Interim Report for Nov.12, 2013 – Jan. 31, 2016**

Distribution A: Approved for public  
release; distribution unlimited. PA Case  
No: TSRL-PA-2016-0302.

**Air Force Research Laboratory  
711th Human Performance Wing  
Airman Systems Directorate  
Bioeffects Division  
Optical Radiation Bioeffects Branch  
JBSA Fort Sam Houston, TX 78234**

## NOTICE AND SIGNATURE PAGE

Using Government drawings, specifications, or other data included in this document for any purpose other than Government procurement does not in any way obligate the U.S. Government. The fact that the Government formulated or supplied the drawings, specifications, or other data does not license the holder or any other person or corporation; or convey any rights or permission to manufacture, use, or sell any patented invention that may relate to them.

Qualified requestors may obtain copies of this report from the Defense Technical Information Center (DTIC) (<http://www.dtic.mil>).

"The Effects of Scattered Light from Optical Components on Visual Function"

(AFRL-RH-FS-TR - 2016 -0018 ) has been reviewed and is approved for publication in accordance with assigned distribution statement.

MCLIN.LEON.N.JR.1034434359

Digitally signed by MCLIN.LEON.N.JR.1034434359  
DN: c=US, o=U.S. Government, ou=DoD, ou=PKI,  
ou=USAF, cn=MCLIN.LEON.N.JR.1034434359  
Date: 2016.08.01 11:41:11 -05'00'

---

LEON N. MCLIN, O.D., M.S.  
Contract Monitor  
Optical Radiation Bioeffects Branch

POLHAMUS.GARR  
ETT.D.1175839484

Digitally signed by  
POLHAMUS.GARRETT.D.1175839484  
DN: c=US, o=U.S. Government, ou=DoD, ou=PKI,  
ou=USAF, cn=POLHAMUS.GARRETT.D.1175839484  
Date: 2016.10.16 12:08:14 -05'00'

---

GARRETT D. POLHAMUS, DR-IV, DAF  
Chief, Bioeffects Division  
Airman Systems Directorate  
711th Human Performance Wing  
Air Force Research Laboratory

This report is published in the interest of scientific and technical information exchange, and its publication does not constitute the Government's approval or disapproval of its ideas or findings.

<b>REPORT DOCUMENTATION PAGE</b>				<i>Form Approved</i> <i>OMB No. 0704-0188</i>	
Public reporting burden for this collection of information is estimated to average 1 hour per response, including the time for reviewing instructions, searching existing data sources, gathering and maintaining the data needed, and completing and reviewing this collection of information. Send comments regarding this burden estimate or any other aspect of this collection of information, including suggestions for reducing this burden to Department of Defense, Washington Headquarters Services, Directorate for Information Operations and Reports (0704-0188), 1215 Jefferson Davis Highway, Suite 1204, Arlington, VA 22202-4302. Respondents should be aware that notwithstanding any other provision of law, no person shall be subject to any penalty for failing to comply with a collection of information if it does not display a currently valid OMB control number. <b>PLEASE DO NOT RETURN YOUR FORM TO THE ABOVE ADDRESS.</b>					
<b>1. REPORT DATE (DD-MM-YYYY)</b> 21-02-2016		<b>2. REPORT TYPE</b> Interim technical Report		<b>1. REPORT DATE (DD-MM-YYYY)</b> Nov.12, 2013 – Jan.31, 2016	
<b>4. TITLE AND SUBTITLE</b> The Effects of Scattered Light from Optical Components on Visual Function				<b>5a. CONTRACT NUMBER</b> FA8650-14-D-65190	
				<b>5b. GRANT NUMBER</b>	
				<b>5c. PROGRAM ELEMENT NUMBER</b> 0603231F	
<b>6. AUTHOR(S)</b> Thomas Kuyk, Peter A. Smith, Solangia Engler, Paul V. Garcia, William R. Brockmeier, Brenda J. Novar, Christopher Putnam and Leon McLin				<b>5d. PROJECT NUMBER</b> 5323	
				<b>5e. TASK NUMBER</b> HD	
				<b>5f. WORK UNIT NUMBER</b> 03/H0BA	
<b>7. PERFORMING ORGANIZATION NAME(S) AND ADDRESS(ES)</b> Engility Corporation 711th Human Performance Wing Airman Systems Directorate Bioeffects Division Optical Radiation Bioeffects Branch				<b>8. PERFORMING ORGANIZATION REPORT NUMBER</b>	
<b>9. SPONSORING / MONITORING AGENCY NAME(S) AND ADDRESS(ES)</b>  711th Human Performance Wing Airman Systems Directorate Directed Energy Bioeffects Optical Radiation Bioeffects Branch				<b>10. SPONSOR/MONITOR'S ACRONYM(S)</b> 711 HPW/RHDO	
				<b>11. SPONSOR/MONITOR'S REPORT NUMBER(S)</b>  AFRL-RH-FS-TR-2016-0018	
<b>12. DISTRIBUTION / AVAILABILITY STATEMENT</b> Distribution A: Approved for public release; distribution unlimited. PA Case No: TSRL-PA-2016-0302					
<b>13. SUPPLEMENTARY NOTES</b>					
<b>14. ABSTRACT</b> Contrast acuity and contrast sensitivity were measured in twelve subjects without and with eight different optical materials (OM) positioned in front of their right eye. The measurements were taken without and with light from a glare source present. The OM consisted of four haze standards with percent haze (H%) between approximately 1 and 20% and four reflective LEP with percent haze between 1 and 5%. In addition to H%, clarity, light scatter (log (s)) at scatter angles between 7-10° and the amount of scatter at angles from 1-70° (bi-directional transmission distribution function or BTDF) were measured. The scatter metrics, H%, log (s), and cumulative scatter beyond specific angles from the BTDF were plotted against changes in contrast acuity and contrast sensitivity between no OM (baseline) and OM viewing conditions with and without glare, which included measured change in visual performance between the Glare and No Glare conditions for each OM. The general effect of glare was to reduce acuity and contrast sensitivity. For the haze standards, H% was an excellent predictor of the performance declines with glare. For the LEP, H% was determined not a good predictor, where scatter metrics derived from the BTDF were found to be the best predictors of the performance losses with glare. The latter finding suggests measurement of the BTDF of reflective LEP provides important information about scatter effects on visual function that the traditional scatter measure of haze does not perform to provide an accurate metric.					
<b>15. SUBJECT TERMS</b>					
<b>16. SECURITY CLASSIFICATION OF:</b> Unclassified			<b>17. LIMITATION OF ABSTRACT</b>  Unclassified	<b>18. NUMBER OF PAGES</b>  26	<b>19a. NAME OF RESPONSIBLE PERSON</b> Brenda Novar
<b>a. REPORT</b> Unclassified	<b>b. ABSTRACT</b> Unclassified	<b>a. REPORT</b> Unclassified			<b>19b. TELEPHONE NUMBER (include area code)</b>

Standard Form 298 (Rev. 8-98)  
Prescribed by ANSI Std. Z39.18

**This Page Intentionally Left Blank**

## TABLE OF CONTENTS

TABLE OF CONTENTS.....	iii
TABLE OF FIGURES.....	iv
LIST OF TABLES.....	vi
1 INTRODUCTION.....	1
2 METHODS.....	2
2.1 Materials.....	2
2.2 Subjects .....	4
2.3 Visual Function Assessment .....	4
2.4 Data Analysis .....	5
3 RESULTS.....	6
3.1 Regan Contrast Acuity .....	7
3.2 Spatial Contrast Sensitivity (SCS) .....	14
4 DISCUSSION.....	18
5 REFERENCES .....	22

## TABLE OF FIGURES

Figure 1. Resolution in minutes of arc visual angle as a function of letter contrast on the Regan charts for the baseline and five LEP used in the study. Solid lines indicate results for the No Glare (NG) condition; dashed lines the Glare (G) condition. Error bars on the baseline functions are $\pm 1$ sd.....	7
Figure 2. Same as Figure 1 except results are for the neutral density filter (NDF) and the four haze standards (Tiles in the legend). Solid lines indicate results for the No Glare (NG) condition; dashed lines the Glare (G) condition. Error bars on the baseline functions are $\pm 1$ sd. The baseline results are the same as shown in Figure 1 .....	8
Figure 3. Data from Figure 1 for the LEP replotted as a function of the reciprocal of letter contrast (contrast sensitivity). Solid lines indicate results for the No Glare (NG) condition; dashed lines the Glare (G) condition. Error bars on the baseline functions are $\pm 1$ sd.....	8
Figure 4. Data from Figure 2 for the haze standards (Tiles) replotted as a function of the reciprocal of letter contrast (contrast sensitivity). Solid lines indicate results for the No Glare (NG) condition; dashed lines the Glare (G) condition. Error bars on the baseline functions are $\pm 1$ sd .....	9
Figure 5. Examples of linear regression fits for the MAR difference from baseline data for the 10% and 20% haze standards (T). The insets show the regression results for slope (y), intercept and correlation ( $R^2$ ).....	10
Figure 6. Examples of linear regression fits for the MAR difference between the No Glare – Glare condition for 10% and 20% haze tiles. The insets show the regression results for slope (y), intercept and correlation ( $R^2$ ) .....	11
Figure 7. Baseline difference function slopes, No Glare condition, for the LEP and haze tiles groups plotted against percent haze. The solid lines are the linear regression lines and insets show the regression results for slope (y), intercept and correlation ( $R^2$ ).....	12
Figure 8. Baseline difference function slopes for the LEP and haze tiles groups, Glare condition, plotted against percent haze. The solid lines are the linear regression lines and insets show the regression results for slope (y), intercept and correlation ( $R^2$ ).....	13
Figure 9. Slopes of the No Glare – Glare (NG-G) difference functions for the LEP and haze standards plotted against percent haze. The solid lines are the linear regression lines and insets show the regression results for slope (y), intercept and correlation coefficient ( $R^2$ ).....	13
Figure 10. SCS function for the LEP in the No Glare (NG) and Glare (G) conditions .....	15
Figure 11. SCS function for the haze standards (Tiles) in the No Glare (NG) and Glare (G) conditions .....	16

Figure 12. The difference in AUF between the baseline and OM's in the Glare condition plotted against haze (%) for the haze standards (Tiles) and LEP .....	17
Figure 13. The differences in AUF between the No Glare and Glare conditions plotted against haze (%) for the haze standards (Tiles) and LEP .....	17

## LIST OF TABLES

Table 1. Scatter metrics for the optical materials (OM) used .....	3
Table 2. Relationships between the scatter metrics for the haze standards and LEP .....	6
Table 3. Haze: Slopes and $R^2$ from the linear regression fits to the baseline MAR difference function and NG-G MAR difference function slope data plotted against percent haze. See text for details and Figure 8-10 for examples that include the same results .....	13
Table 4. BTDF: Slopes and $R^2$ from the linear regression fits to the baseline MAR difference function and NG-G MAR difference function slope data plotted against scatter $>15^\circ$ for LEP and scatter $>2^\circ$ for haze tiles. See text for details and Figure 8-10 for examples .....	14
Table 5. Log (s): Slopes and $R^2$ from the linear regression fits to the baseline MAR difference function and NG-G MAR difference function slope data plotted against C-Quant log (s). See text for details and Figure 8-10 for examples .....	14
Table 6. Haze: Slopes and $R^2$ from the linear regression fits to the baseline AUF difference function and NG-G AUF difference function slope data plotted against percent haze. ....	18
Table 7. BTDF: Slopes and $R^2$ from the linear regression fits to the baseline AUF difference function and NG-G AUF difference function slope data plotted against scatter $>2^\circ$ , $>12^\circ$ and $>12^\circ$ for LEP and scatter $>2^\circ$ , $>15^\circ$ and $>8^\circ$ for haze tiles for the three comparisons, respectively. * Indicates virtual tie with $R^2$ for same comparison with log (s) in Table 7 .....	18
Table 8. Log (s): Slopes and $R^2$ from the linear regression fits to the baseline AUF difference function and NG-G AUF difference function slope data plotted against C-Quant log (s). * Indicates virtual tie with $R^2$ for same comparison with BTDF in Table 6 .....	18



# 1 INTRODUCTION

The operational threat from lasers and the subsequent need for human protection, most notably from vision loss, has been recognized by the military since the 1980's. Laser eye protection (LEP) provides a means to mitigate the impact of laser illumination of the eye, the effects of which range from temporary visual disruption to permanent damage. LEP works by preventing laser light from reaching the eye, either by absorbing it or reflecting it away from the eye. All LEP currently in use by the Air Force incorporate absorptive dyes and/or reflective coating technologies. However, blocking laser light in the visible spectrum unavoidably reduces the total amount of light available for visual sensing and performance function and may cause unwanted visual effects such as reduced image contrast or changes in the appearance of colored stimuli. [1]

Another potential source of visual performance degradation from eyewear, including LEP, is light scatter, often referred to as haze. Haze is typically measured as the ratio of light scattered to the light transmitted through an optical component. In general, as the amount of haze increases, visual acuity and contrast sensitivity decrease, and this may be exacerbated when a glare source, such as sunlight or a bright light at night is present.

To preserve visual performance, current standards for aircrew LEP specify that haze be less than 3% of incident light intensity. [2] However, several studies found that in the presence of an external glare source, the relationship between the amount of haze in an LEP and visual acuity was not the same for the absorptive and reflective technology types [3, 4]. For absorptive type LEP, the rate of decline in acuity with increasing haze paralleled that of a set of haze standards. For reflective LEP, the rate of decline with increasing haze was significantly faster compared to the haze standards or the absorptive LEP. [4] Furthermore, the performance decline occurred for reflective LEP that met the Air Force's haze requirement (<3%). This finding supports anecdotal reports of user rejection of reflective LEP that meet the haze requirement (Byron Edmonds and Gregg Irvin, personal communication, March 2015) and suggests another factor unique to reflective technologies is involved that the haze measurement does not account for in operator visual performance.

An additional factor for visual performance decrements may be differences in how the light is scattered at different angles by the LEP, which is presently not captured by the haze measurement [5]. Haze is a measure of total amount of light scattered beyond an angle of  $2.5^\circ$  and is therefore a measure of wide angle scatter [6]. The amount of light scattered over a narrow angle  $<2.5^\circ$  is used as an index of the "see through quality" or the clarity of an optical component. For the most part, LEP developed by the US Air Force possess uniformly high clarity, on the order of 97-100%, and clarity differences are not likely to account for the accelerated decline in acuity observed using reflective LEP in the presence of a glare source. However, the distribution of light scatter in an optical material as a function of angle is not always uniform, [5] and neither the haze nor clarity metrics capture these non-uniformities. Some recent observations by Gregg Irvin (personal communication, September 2014) suggest a non-uniform distribution of scatter in reflective LEP, with relatively more scatter at higher

scatter angles, which may be related to the reduction of acceptability in terms of operator subjective judgements of haze and visibility through the LEP. A better idea of whether or not haze is uniformly or non-uniformly distributed may be achieved by assessing light scatter at intermediate angles. This metric can be evaluated using a device called the C-Quant. The C-Quant is a commercially available clinical ophthalmic instrument (Oculus Optikgerate GmbH, Wetzlar, Germany) that measures light scatter in the human eye (intraocular scatter) over a region from  $\sim 5^\circ$  -  $10^\circ$  from the optical axis, or at an average scatter angle of approximately  $7^\circ$ . [7] Although the C-Quant instrument was not specifically designed to measure light scatter in optical components, applying it to measure light scatter with and without an optical component in front of the eye and then calculating the difference, may provide data to derive a measure of intermediate angle scatter of a LEP system. The amount of intermediate angle scatter may be associated with visual performance either by itself or in combination with the haze and/or clarity measures.

Adding a measure of intermediate angle scatter may or may not provide all of the information required to the associate LEP light scatter issues causing changes in visual function. For example, it may be that the amount of light scattered between  $10^\circ$  and  $20^\circ$  is more important in terms of visual acceptance and performance in the presence of glare than in the  $5$ - $10^\circ$  zone assessed with the C-Quant. What may be needed is a graded measurement of the complete angular distribution of light scatter in an optical material in the form of the bi-directional transmission distribution function (BTDF). This BTDF data could be used to determine if more or less scatter in specific angular zones (e.g.,  $0$ - $5^\circ$  vs  $5$ - $10^\circ$ ) occurs, then the general distribution of scatter, uniform or not, or that some ratio of scatter between different angular zone relates best to visual function changes in glare. However, for best use of BTDF information as a predictor of visual performance, these metrics must be developed to evaluate relevant contributing scatter aspects when applying BTDF.

In this study, visual performance was measured from human observers with nothing in front of the eyes as well as the subjects looking through different type of optical materials (OM) including haze standards, reflective type LEP, and a neutral density filter (NDF). Light scatter in the OM was also measured using the differentiating techniques described above; haze, clarity, C-Quant, and BTDF, and these measures were evaluated for their ability to predict changes in individual human visual performance measures. In addition, the measures of scatter were evaluated in a multi-predictor statistical model to determine if combining measures will provide better accounts for effects on visual performance compared to any single measure.

## **2 METHODS**

### **2.1 Materials**

The OM used in this study included four haze standards, four LEP of the reflective type, and one NDF. The haze standards were glass plates with particles suspended in them to yield different levels of haze between approximately 0.2 and 20% (BYK Gardner). The four reflective LEP included three US Air Force prototypes; two of the same type that differed in haze, A-LH (type

A low haze) and A-HH (type A high haze) and an older type B with no blocking of visible wavelengths (B0), as well as one commercially available LEP manufactured by Iridian (NTU-10). The NDF was a Kodak Wratten #96 gelatin-type filter with a photopic luminous transmittance (PLT) of approximately 40%. It was selected to match the PLT of the lowest transmission NTU-10 LEP and was used as a control to determine the effect of light reduction on the visual performance measurements. The haze standards, several of the LEP consisting of a single lens element, and the NDF were mounted in custom-made holders similar to eyeglass frames that could be fit to a subject's head with the optical material located in front of one eye. Two of the LEP were already in spectacle formats and were used as is during the experiment.

Physical measurements made on the OM included PLT, wide-angle light scatter or haze, narrow-angle light scatter or clarity, light scatter at an intermediate angle (C-Quant) and the bi-directional transmission distribution function (BTDF), which is a measure of light scatter at scatter angles from 0° to 70°. PLT was measured with a Cary 6000i spectrophotometer through the center of each optical element. Haze and clarity were measured with a BYK Haze-Guard Plus according to the American Society for Testing and Materials (ASTM) guidelines.[6] Intermediate angle scatter was measured with the C-Quant using human subjects as the detector. The C-Quant is normally used to assess intraocular scatter in the human eye.[7,8] In our application, a measurement was taken without and then with an OM in front of the eye and the difference in the amount of scatter between the naked eye and eye plus OM was used as the measure of intermediate angle scatter. The BTDF for each OM was measured using a custom-built scatterometer. The primary metric used in the analysis was the cumulative scatter beyond specific scatter angles. Other BTDF metrics that were evaluated included cumulative scatter at scatter angles less than a specified angle and the ratio of scatter between narrow and wide angles. Table 1 lists the PLT and scatter metrics for all of the optical materials. The "Scatter 8" metric is derived from the BTDF. It is one of many that could be used and represents the total amount of scatter for angles greater than 8°.

**Table 1. Scatter metrics for the optical materials (OM) used**

<b>OM</b>	<b>PLT</b>	<b>HAZE</b>	<b>CLARITY</b>	<b>C-QUANT</b>	<b>SCATTER 8</b>
<b>HAZE 1</b>	94.0	0.21	99.8	-0.005	0.0068
<b>HAZE 5</b>	94.1	3.84	99.6	0.030	0.2739
<b>HAZE 10</b>	93.5	10.90	99.1	0.469	1.1029
<b>HAZE 20</b>	93.0	19.70	98.3	0.814	1.9504
<b>B0</b>	93.2	0.88	100.0	0.043	0.0408
<b>A-LH</b>	86.8	1.77	93.0	0.039	0.1069
<b>A-HH</b>	82.4	5.04	97.0	0.157	0.2267
<b>NTU-10</b>	46.1	4.09	99.7	0.094	0.0948
<b>NDF</b>	39.8	0.50	99.5	0.015	0.0066

## 2.2 Subjects

Ten adults participated in the study, seven were male and three were female (mean age =  $29.6 \pm 8.6$  years). They all had visual acuity equal to or better than 20/25 corrected or uncorrected in each eye, normal color vision (Ishihara test and Standard Pseudoisochromatic Plates, Part 2), and no self-reported vision problems. Observers were also not taking any medications that might affect the sensitivity of the eye and none reported having refractive surgery within the past year (photorefractive keratectomy (PRK) or laser-assisted in situ keratomileusis (LASIK)). They performed all the visual function tasks monocularly, using the right eye.

## 2.3 Visual Function Assessment

Contrast acuity (CA) was assessed with the Regan test [9] and spatial contrast sensitivity (SCS) with Gabor sine wave stimuli displayed on a computer monitor. The CA and SCS measurements were made with and without the OM's in front of the eye, with and without a glare light source present. The source of the glare was the Brightness Acuity Tester (BAT). The BAT is a commercially available ophthalmic device that has been used in previous studies to provide a monocular glare source of approximately 7,000 lux.[3,4]

The Regan contrast acuity test consists of five printed charts, each containing rows of eight greyscale letters on a white background. The size of the letters decreases from the top row to the bottom row. Subjects progress down the chart until they can no longer read any letters on a line. Guessing was encouraged and the total number of letters correctly read was recorded. Correctly reading more letters (rows with smaller letters) indicates that the observer can resolve smaller visual angles (higher acuity). Each chart has letters of a single contrast and the battery includes charts with letters at 96%, 50%, 25%, 11%, or 4% contrast, allowing acuity to be measured for a wide range of contrast levels. The charts were illuminated by overhead fluorescent room lighting that yielded a luminance of the white areas of the charts of approximately  $105 \text{ cd} \cdot \text{m}^{-2}$ , which is in the recommended range for the test of between 80 and  $300 \text{ cd} \cdot \text{m}^{-2}$ . Contrast acuity was assessed monocularly with an opaque black eye patch covering the other eye during testing.

Contrast sensitivity was measured using a Visage visual stimulus generator with Metropsis software and a 60-cm Boldscreen LCD display (Cambridge Research Systems, Cambridge, U.K). The display was placed 6 m from the observer, and used a video resolution of  $1920 \times 1080$  pixels and an average luminance (dark plus light sine wave bar/2) of  $100 \text{ cd} \cdot \text{m}^{-2}$ . Vertical achromatic Gabor patches subtending  $5^\circ$  centrally, with sinusoidal gratings of 1.0, 2.0, 4.0, 8.1, and 16.1 cycles per degree (cpd) were used as stimuli. All subjects started SCS session with contrast levels selected during piloting of 20% for 1 cpd and 8.1 cpd, 10% for 2 cpd and 4 cpd and 50% for the high spatial frequency of 16.2 cpd. A two-alternative temporal forced-choice psychophysical procedure was used, where the subject's task was to identify whether the stimulus was presented on the screen during the first or second of two 1-s intervals, and to press the left ("first") or right ("second") button on a response box. Targets were randomly presented

in one of the intervals. Target presentation was for 500 ms within a raised cosine temporal envelope of 1-s.

A dynamic psychophysical staircase with logarithmic steps was used. The stimulus contrast for each spatial frequency started at a level that would be easily detected based on initial pilot tests. At the beginning of the test, the stimulus contrast decreased 1.5 dB after every correct response. After the first incorrect response, the staircase started a more strict criteria and the stimulus contrast increased by 0.4 dB after every incorrect response and decreased 0.3 dB after every correct response. During the test the five spatial frequencies were randomly interleaved, and the session ended after six response reversals were recorded for each spatial frequency tested. The thresholds were calculated by averaging the contrast values of the last four response reversals for each grating, and contrast sensitivity was estimated as the reciprocal of the threshold values.

## 2.4 Data Analysis

The experimental design was a within-subjects design with results analyzed using a within-subject analysis of variance (ANOVA). The independent variables for contrast acuity ANOVA were Letter Contrast, Glare (No Glare/Glare), and Optical Material (including no optical material). Separate analyses were completed for the haze standards and the LEP as well as an analysis that combined both conditions. The dependent variable was visual acuity measured in minimum visual angle. The same set of ANOVA's was completed for contrast sensitivity data with Spatial Frequency, Glare, and Optical Material as the independent variables and SCS as the dependent variable.

In addition to the ANOVA, for the contrast acuity data, the decrement in minimum angle of resolution (MAR) in minutes of arc between the baseline and each optical material (OM) condition was determined at each letter contrast for the No Glare and Glare conditions. The MAR differences were then plotted as a function of 1/contrast and linear regression was used to obtain the slope of the difference functions for each OM for the No Glare and Glare conditions. The slope values for each OM were then replotted as a function of the value of a scatter metric for each filter for the No Glare and Glare conditions. In the plots the results for the haze standards and LEP were treated as separate groups following Dykes *et al.*[4]

The contrast sensitivity data were treated similarly except that rather than determine differences at each spatial frequency between baseline and each filter condition, the area under the contrast sensitivity function (AUF) was determined for each trial and then the area differences from baseline were determined for each OM for the No Glare and Glare conditions. The area differences from baseline were then plotted as a function of a scatter metric for the No Glare and Glare conditions separately. As with the MAR, the haze standards and LEP were treated as separate groups. The glare condition is of particular interest as this is where a significant difference in the slopes of the contrast acuity decrement versus haze functions between the reflective LEP and haze standards was previously found.[4]

Another analysis was also completed using the MAR and AUF results, but rather than compare filter results to baseline, the differences in MAR or AUF between the No Glare and Glare conditions (NG-G) was determined for each OM and plotted as functions of the scatter metrics. The method for doing this for the MAR and AUF was slightly different. For the MAR, the decrement between the No Glare and Glare conditions was determined at each letter contrast for each OM and the differences (in MAR) plotted as a function of 1/letter contrast. Linear regression was used to obtain the slope of the difference function for each OM. The slope data were then plotted as a function of each of the scatter metrics (haze, BTDF scatter greater than  $x^\circ$ , and C-Quant log (s)) and linear regression used to derive correlation data and determine which metric best predicted the loss of acuity in the presence of glare. The analysis was simpler for the contrast sensitivity data since AUF summarizes the entire function so the NG-G difference for each filter condition was simply plotted as a function of the haze metrics. For both MAR and AUF NG-G data sets, the haze tiles and LEP were treated as different groups. Multiple regression analysis was subsequently used to determine if any one light scatter metric or a combination of metrics best accounted for the contrast acuity or contrast sensitivity decrements with glare.

### 3 RESULTS

As a first step in the analysis, the degree of correlation between the scatter metrics was determined and those results are shown in Table 2. For both the tiles and LEP percent haze was strongly correlated with both the C-Quant metric, log (s), and the total amount of scatter at scatter angles of greater than  $3^\circ$ . The relationship between log (s) and BTDF scatter was also very strong for the haze standards for total BTDF scatter at angles greater than  $15^\circ$ . There was also a moderately strong association between log (s) and BTDF for the LEP but the amount of angular scatter that provided the highest  $R^2$  was the total scatter at  $>3^\circ$ . The BTDF metric of total scatter  $>3^\circ$  accounts for the majority of all light scatter in the samples, whereas scatter  $>15^\circ$  is a measure of scatter at more peripheral light scatter. The high correlation for all of the pairs for the haze standards suggests nearly equivalent results in predicting performance on the Regan and SCS will be obtained with the three scatter metrics. For the LEP, the results suggest that haze and BTDF scatter  $> 3^\circ$  will yield similar levels of prediction and that log (s) will be likely be less effective.

**Table 2. Relationships between the scatter metrics for the haze standards and LEP**

Correlation Pair	Haze Standards $R^2$	LEP $R^2$
Haze/log (s)	0.973	0.873
Haze/ Scatter BTDF ( $>3^\circ$ )	0.998	0.952
log (s)/Scatter BTDF ( $>15^\circ$ )	0.954	0.768

### 3.1 Regan Contrast Acuity

The contrast acuity results, in number of letters read on the charts at each letter contrast, was converted to acuity expressed as MAR in minutes of arc. Lower numbers indicate better acuity. Figure 1 shows the results for the No Glare and Glare conditions for the LEP and Figure 2 shows the results for the haze standards (referred to as Tiles in all figures). Figure 3 and Figure 4 show the same data but plotted as a function of 1/letter contrast (contrast sensitivity). Converting letter contrast to contrast sensitivity accounts for the non-linear response of the visual system to contrast and also allows for better visualization and comparison of the results.

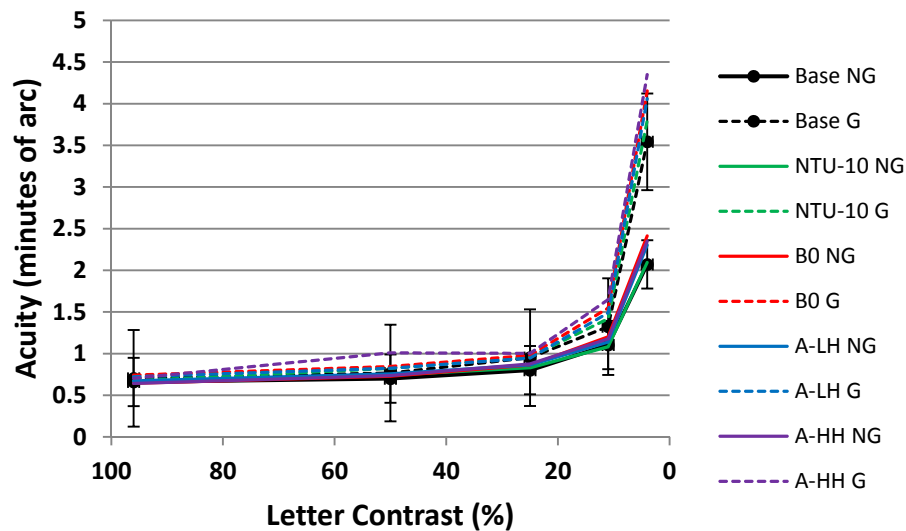


**Figure 1. Resolution in minutes of arc visual angle as a function of letter contrast on the Regan charts for the baseline and five LEP used in the study. Solid lines indicate results for the No Glare (NG) condition; dashed lines the Glare (G) condition. Error bars on the baseline functions are  $\pm 1$  sd**

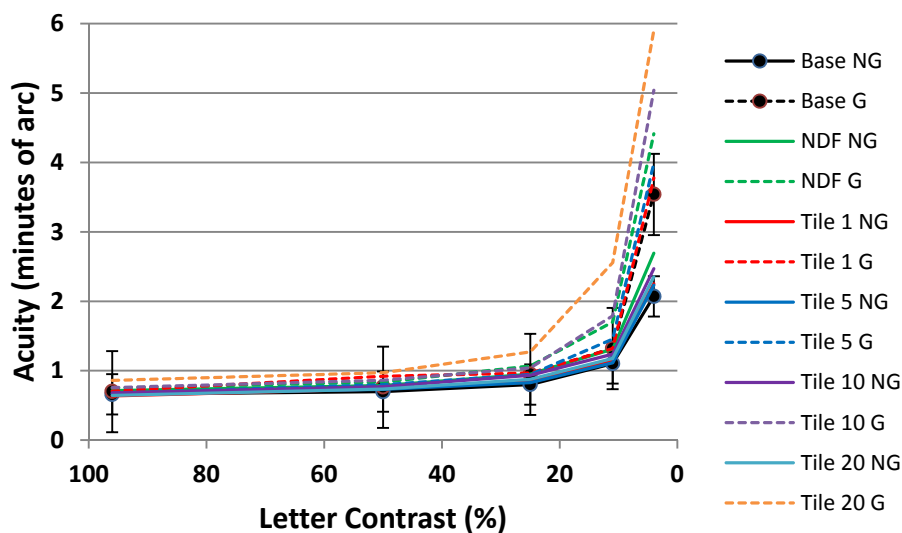


Figure 2. Same as Figure 1 except results are for the neutral density filter (NDF) and the four haze standards (Tiles in the legend). Solid lines indicate results for the No Glare (NG) condition; dashed lines the Glare (G) condition. Error bars on the baseline functions are  $\pm 1$  sd. The baseline results are the same as shown in Figure 1

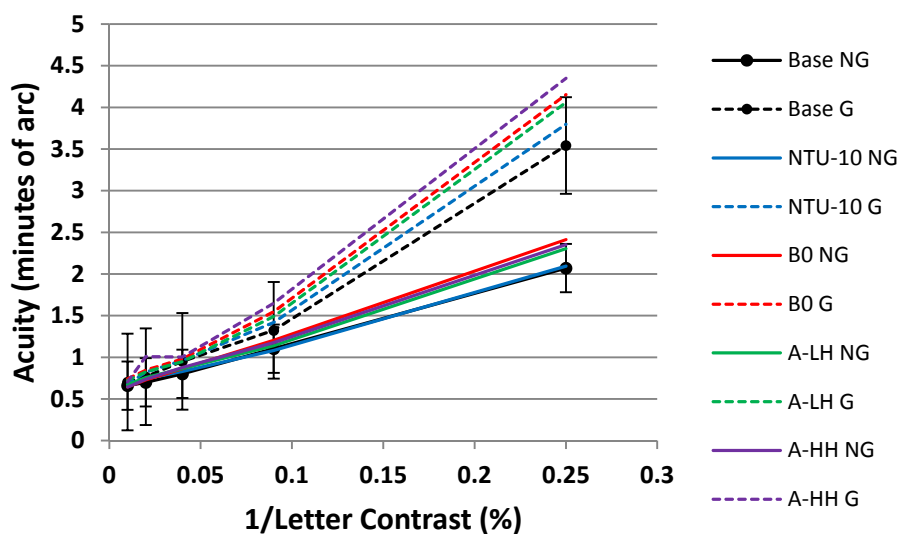
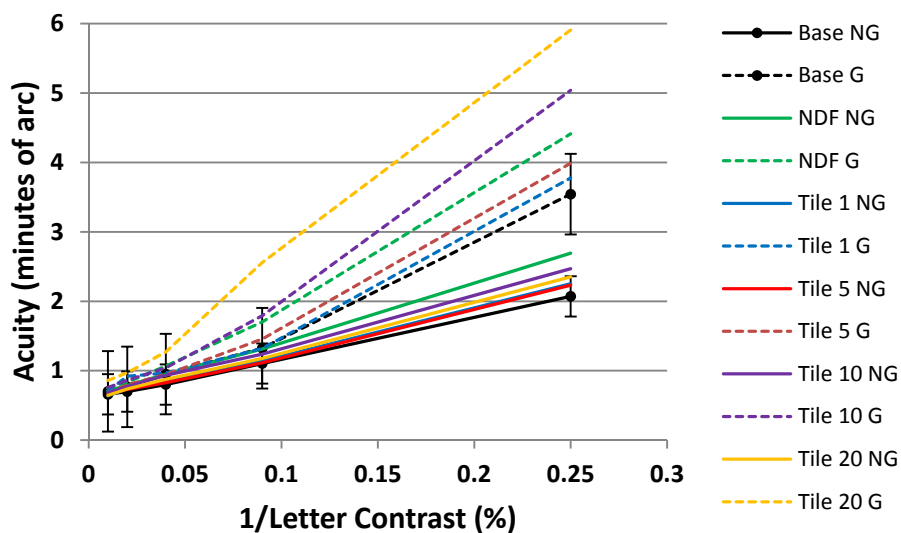


Figure 3. Data from Figure 1 for the LEP replotted as a function of the reciprocal of letter contrast (contrast sensitivity). Solid lines indicate results for the No Glare (NG) condition; dashed lines the Glare (G) condition. Error bars on the baseline functions are  $\pm 1$  sd





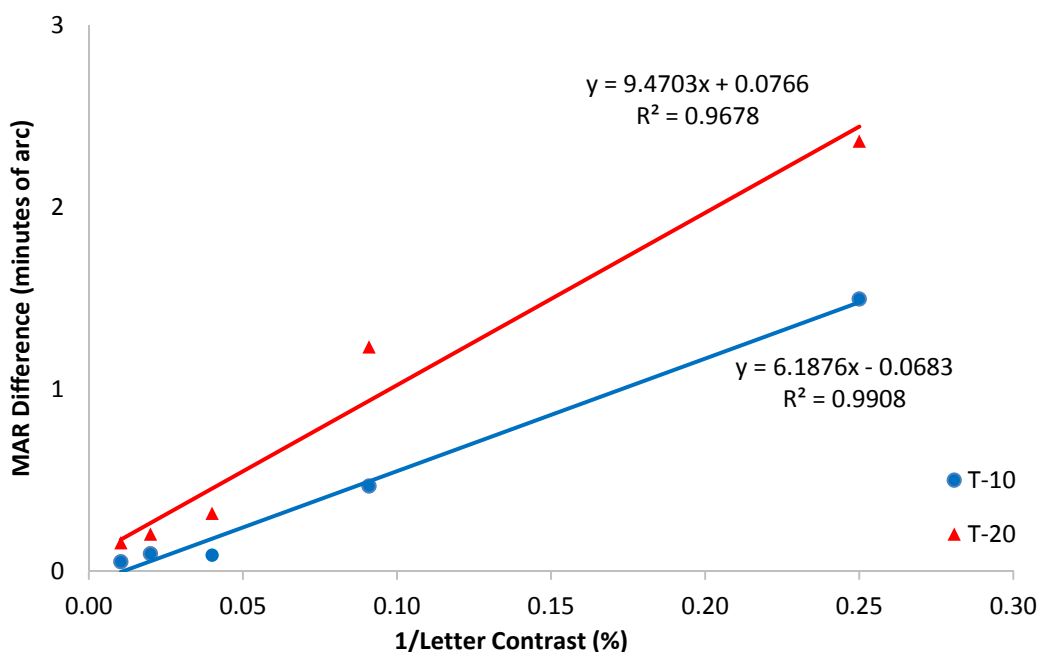
**Figure 4. Data from Figure 2 for the haze standards (Tiles) replotted as a function of the reciprocal of letter contrast (contrast sensitivity). Solid lines indicate results for the No Glare (NG) condition; dashed lines the Glare (G) condition. Error bars on the baseline functions are  $\pm 1$  sd**

Figure 3 and Figure 4 illustrate the main effects of letter contrast, glare, and OM. For both the No Glare and Glare conditions, as letter contrast decreased so did acuity, and this was true for both the LEP ( $F(1.5,13.3)= 430.030$ ,  $p< 0.001$ ) and the haze standards ( $F(1.6,14.3)= 400.638$ ,  $p< 0.001$ ). The impact of adding glare was to significantly reduce acuity compared to the No Glare condition, primarily at the lower letter contrasts. Starting at about 25% letter contrast, acuities for the Glare condition begin to separate from the No Glare results for both the LEP  $F(1,9)= 31.003$ ,  $p< 0.001$  and haze standards  $F(1,9)= 43.166$ ,  $p< 0.001$ . This resulted in glare functions with steeper slopes and a significant interaction effect between letter contrast and glare for the LEP ( $F(4,36)= 25.620$ ,  $p< 0.001$ ) and haze standards ( $F(4,36)= 41.461$ ,  $p< 0.001$ ).

The significant main effect of OM (LEP,  $F(1,9)= 6.307$ ,  $p= 0.033$ ; haze standards,  $F(1,9)= 15.138$ ,  $p= 0.004$ ) occurred because acuity for the baseline no filter condition was generally better than with LEP or the haze standards. Although the separation of acuity from baseline with the LEP is greater at the lowest letter contrast in the Glare condition that did not result in significant interactions between OM and contrast or between OM, contrast, and glare. For the haze standards, however, acuity clearly separated from baseline at lower letter contrasts (filter\*contrast  $F(2.05,18.45)= 3.679$ ,  $p= 0.044$ ). At the same time, the three-way interaction was not significant; indicating the separation in the No Glare and Glare conditions maintained the same ordering of the haze standards by largest to smallest differences. Finally, difference in acuity between baseline and OM is larger in the Glare than No Glare condition and that is reflected in significant interactions between OM and glare for the LEP  $F(1,9)= 5.330$ ,  $p= 0.046$

and haze standards  $F(1,9) = 14.415$ ,  $p = 0.004$ ). The NDF was not included in the ANOVA, but contrast acuity results obtained with it are included in Figure 2 and Figure 4.

As described earlier, the next step was to determine differences in MAR between baselines and the OMs for the No Glare and Glare conditions as well as the differences in MAR between the No Glare and Glare conditions for each OM. The difference data were then plotted as a function of  $1/\text{contrast}$  and the slopes and goodness of fits were determined using linear regression. Examples for the MAR differences between baseline and OMs in the Glare condition are shown for the 10% and 20% haze standard tiles in Figure 5. The slope data for each OM were then replotted as a function of each of the scatter metrics for the No Glare and Glare conditions, with LEP and haze standards treated as separate groups.



**Figure 5. Examples of linear regression fits for the MAR difference from baseline data for the 10% and 20% haze standards (T). The insets show the regression results for slope (y), intercept and correlation ( $R^2$ )**

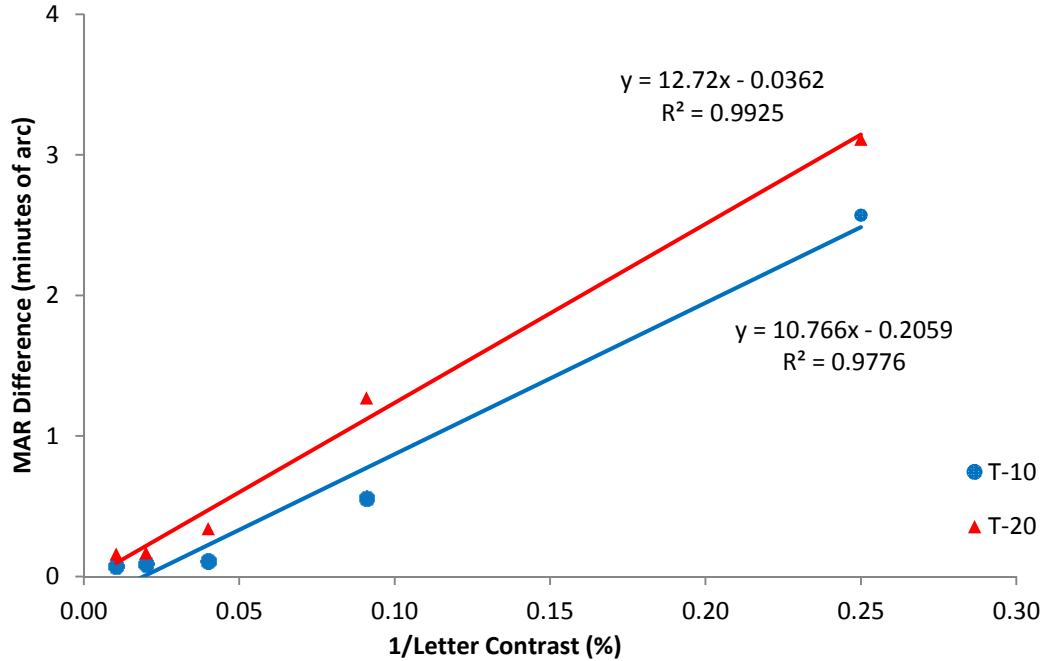


**Figure 6. Examples of linear regression fits for the MAR difference between the No Glare – Glare condition for 10% and 20% haze tiles. The insets show the regression results for slope (y), intercept and correlation ( $R^2$ )**

The difference function slope data for the LEP and the haze tiles treated as separate groups were then plotted against each of the haze metrics, and the resulting functions fit by linear regression. Figure 7 and Figure 8 show the difference from baseline function slopes plotted against % haze for the No Glare and Glare conditions, respectively. The haze tiles group showed a positive correlation for both Glare conditions, and the fit was very good overall ( $R^2 > 0.93$ ). In contrast the fit for the LEP group overall was poor ( $R^2 < 0.012$ ) and had a negative slope in the No Glare condition and a slope near zero in the Glare condition.

Figure 9 shows the NG-G difference function slopes for the same two filter groups. For the haze tiles the correlation coefficient was very high ( $R^2 = 0.97$ ) and moderate for the LEP at 0.43. The slopes of both functions were greater than zero with the haze standard slope being approximately twice that of the LEP group.

Similar fits to those shown in Figure 7 to Figure 9 were completed with BTDF measurements and  $\log(s)$  as the scatter metrics against which the slope data were plotted and linear regression fits calculated. Rather than show a large number of graphs, the slope and  $R^2$  data are summarized in Table 3, Table 4, and Table 5. Table 3 contains the results for the percent haze metric example that were described for Figure 7 to Figure 9, Table 4 shows the results for scatter metrics derived from the BTDF and Table 5 shows the results for  $\log(s)$ .

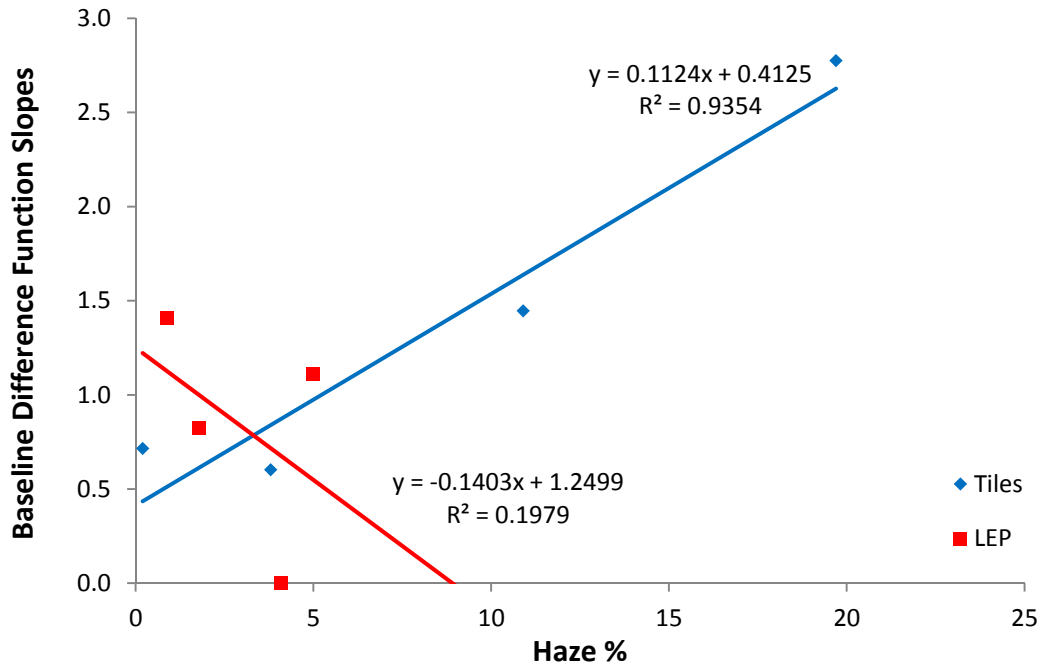
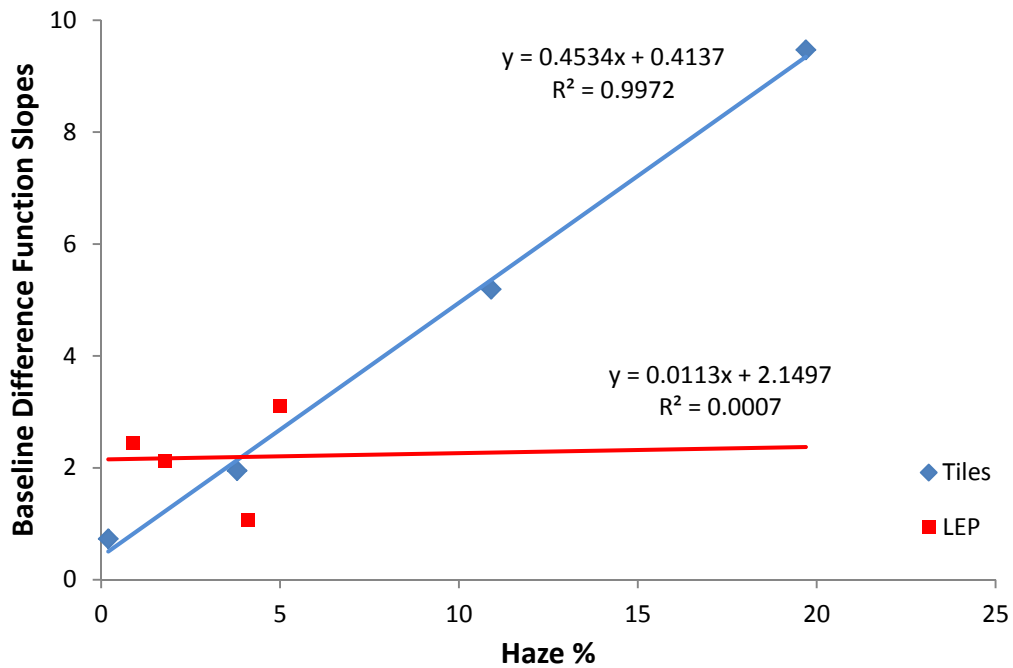
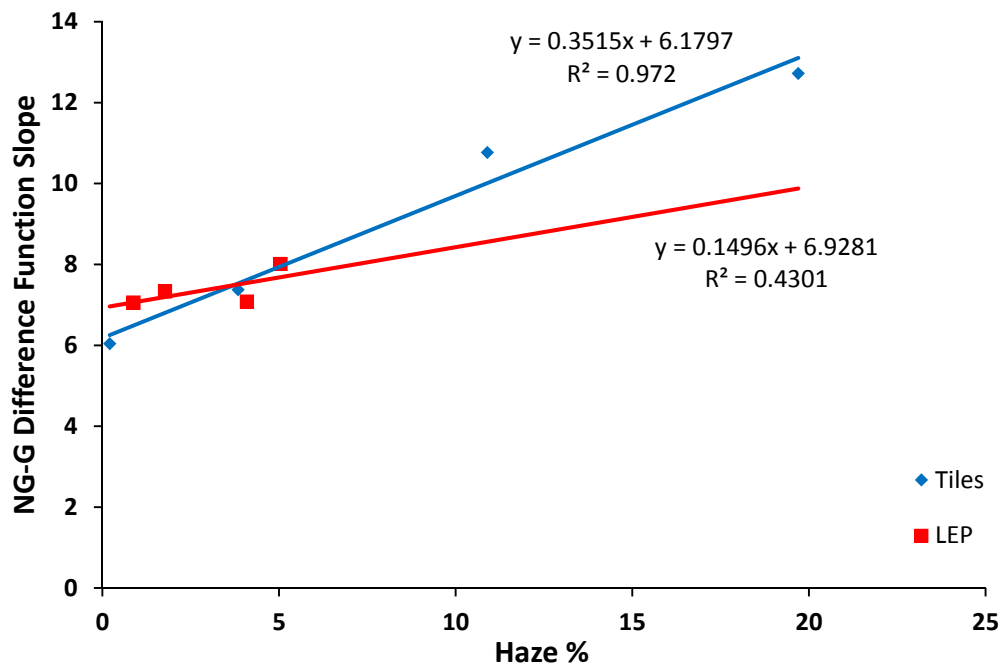


Figure 7. Baseline difference function slopes, No Glare condition, for the LEP and haze tiles groups plotted against percent haze. The solid lines are the linear regression lines and insets show the regression results for slope (y), intercept and correlation ( $R^2$ )



**Figure 8. Baseline difference function slopes for the LEP and haze tiles groups, Glare condition, plotted against percent haze. The solid lines are the linear regression lines and insets show the regression results for slope (y), intercept and correlation ( $R^2$ )**



**Figure 9. Slopes of the No Glare – Glare (NG-G) difference functions for the LEP and haze standards plotted against percent haze. The solid lines are the linear regression lines and insets show the regression results for slope (y), intercept and correlation coefficient ( $R^2$ )**

In general the difference slope data for the haze tiles were well fit by any of the scatter metrics although the lowest  $R^2$  were obtained using percent haze for the baseline differences, but with scatter  $>2^\circ$  derived from the BTDF for the NG-G difference. Another feature of the data for the haze tiles is that the lowest  $R^2$  values for all metrics were for the baseline difference data for the No Glare condition. For the LEP, no metric was a good predictor of the baseline difference function data in the No Glare condition. For both the baseline difference function data in the Glare condition and the NG-G differences, the scatter  $>15^\circ$  metric derived from the BTDF data provided the best fits to the LEP results.

**Table 3. Haze: Slopes and  $R^2$  from the linear regression fits to the baseline MAR difference function and NG-G MAR difference function slope data plotted against percent haze. See text for details and Figure 8-10 for examples that include the same results**

		BASE DIFF NO GLARE	BASE DIFF GLARE	NG-G DIFF
<b>LEP</b>	Slope	0.140	0.011	0.150
	$R^2$	<b>0.179</b>	0.0007	0.430
<b>TILES</b>	Slope	0.112	0.453	0.352
	$R^2$	<b>0.935</b>	<b>0.997</b>	0.972

**Table 4. BTDF: Slopes and  $R^2$  from the linear regression fits to the baseline MAR difference function and NG-G MAR difference function slope data plotted against scatter  $>15^\circ$  for LEP and scatter  $>2^\circ$  for haze tiles. See text for details and Figure 8-10 for examples**

		BASE DIFF NO GLARE	BASE DIFF GLARE	NG-G DIFF
<b>LEP</b>	Slope	2.24	8.56	6.35
	$R^2$	0.065	<b>0.491</b>	<b>0.986</b>
<b>TILES</b>	Slope	0.172	0.695	0.544
	$R^2$	0.923	0.992	<b>0.987</b>

**Table 5. Log (s): Slopes and  $R^2$  from the linear regression fits to the baseline MAR difference function and NG-G MAR difference function slope data plotted against C-Quant log (s). See text for details and Figure 8-10 for examples**

		BASE DIFF NO GLARE	BASE DIFF GLARE	NG-G DIFF
<b>LEP</b>	Slope	-1.21	5.185	6.39
	$R^2$	0.012	0.115	0.631
<b>TILES</b>	Slope	2.67	11.10	8.65
	$R^2$	0.846	0.956	0.945

Within each OM type, LEP or haze tiles, looking across all three tables, the “best predictor” (highest  $R^2$ ) for each difference comparison method is shown in bold. For the LEP, haze was the best predictor for the difference between the baseline and No Glare condition while BTDF was best for the other two differences. For the haze standards, percent haze was the best predictor of performance for the difference between the baseline and No Glare condition, and between baseline and Glare condition while BTDF was the best predictor for the NG-G difference. Although log (s) provided good prediction of performance for the difference functions where glare was involved it was never the best predictor among the three types of scatter metrics.

### 3.2 Spatial Contrast Sensitivity (SCS)

The results of the SCS test for the LEP and haze standards plus NDF groups are shown in Figure 10 and Figure 11, respectively. The results for the No Glare condition are plotted as solid lines and the for the Glare condition as dashed lines. The ANOVA revealed no significant main effect of OM for either the LEP or haze standards. There were, however significant effects of Glare and Spatial Frequency. The Glare effect for the LEP ( $F(1,9)= 14.512$ ,  $p= 0.004$ ) and the haze standards ( $F(1,9)= 22.035$ ,  $p= 0.001$ ) is easily observed in Figure 10 and Figure 11, where the functions for the Glare condition generally lie well below the functions for the No Glare condition on the sensitivity axis. The main effect of spatial frequency was expected; the SCS functions are characterized by having greater sensitivity at mid spatial frequencies than at low and high spatial frequencies. Finally, there was a significant interaction effect between Spatial Frequency and Glare for both the LEP ( $F(3.7,22.3)= 3.670$ ,  $p= 0.016$ ) and haze standards ( $F(3.4, 30.3)= 5.027$ ,  $p= 0.005$ ). The interaction indicates that the decline in sensitivity with glare was

not of the same magnitude at all spatial frequencies. For the LEP (Figure 11) it appears as though the loss at the highest spatial frequency was less than at several of the lower spatial frequencies. For the haze standards, the loss at the two highest spatial frequencies appears to be smaller than the loss at lower frequencies.

The generalized loss of sensitivity with glare resulted in significant changes in the AUF for all test conditions. Like the analysis of the contrast acuity data, two types of comparisons were completed. The first comparison looked at the differences in filter AUF compared to baseline for the No Glare and Glare conditions, while the second compared the difference in AUF between the No Glare and Glare conditions (NG-G) for each OM.

The LEP and haze standard AUF differences from baseline for the Glare condition are plotted in Figure 12 against percent haze to illustrate some of the results, and the linear regression fits to the data. Similarly, Figure 13 shows an example of the LEP and haze standard differences in AUF between the NG-G conditions plotted against percent haze, and the linear regression fits to the data.

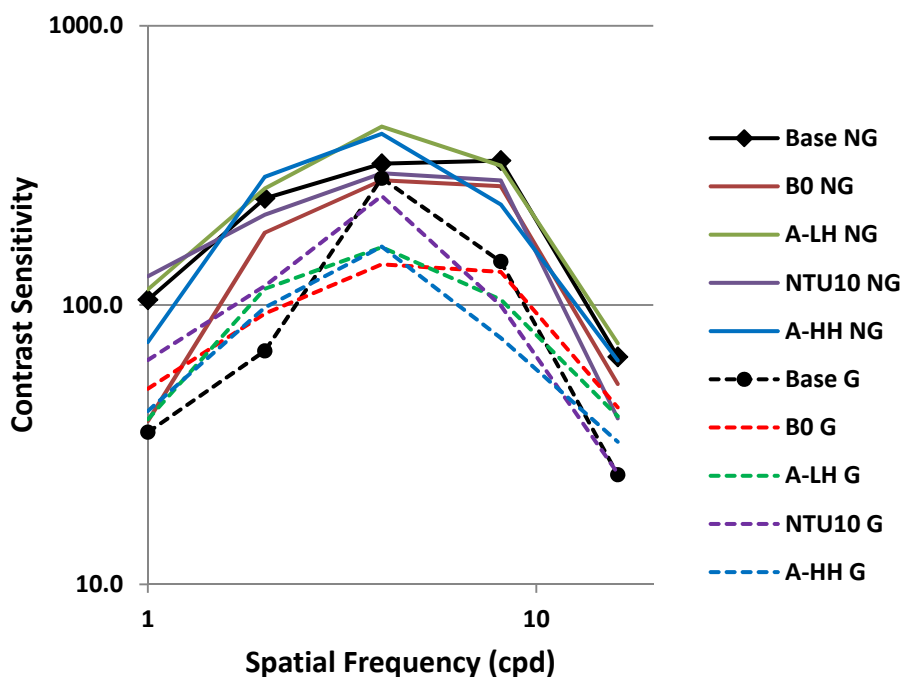
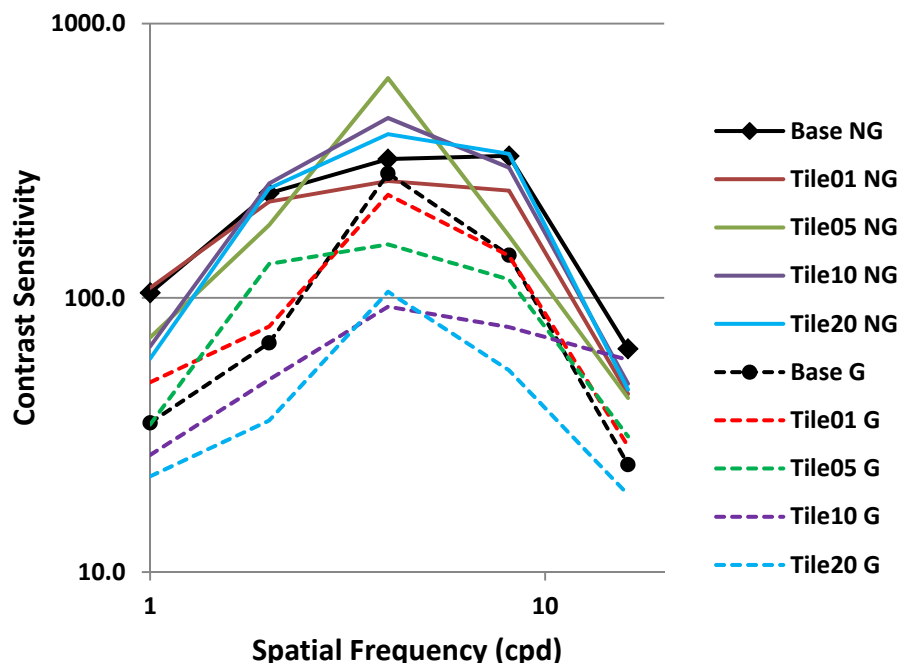


Figure 10. SCS function for the LEP in the No Glare (NG) and Glare (G) conditions



**Figure 11. SCS function for the haze standards (Tiles) in the No Glare (NG) and Glare (G) conditions**

All of the linear fit results for the AUF differences from baseline, No Glare and Glare conditions, and the NG-G within filter comparison are summarized for the scatter metrics, percent haze, BTDF scatter, and  $\log(s)$  in Table 6, Table 7, and Table 8. For the haze standards, all of the scatter metrics provided good fits to the data for comparisons in the Glare condition with BTDF providing the best ( $R^2 \geq 0.98$ ). For the LEP, the best fit for Glare condition comparisons was obtained with the scatter metric derived from the BTDF, although  $\log(s)$  was nearly as good for the baseline to LEP comparison for the Glare condition. For the baseline to LEP comparison for the No Glare condition, none of the metrics provided good prediction of the results with the highest  $R^2 = 0.105$  was given by the  $\log(s)$  metric.



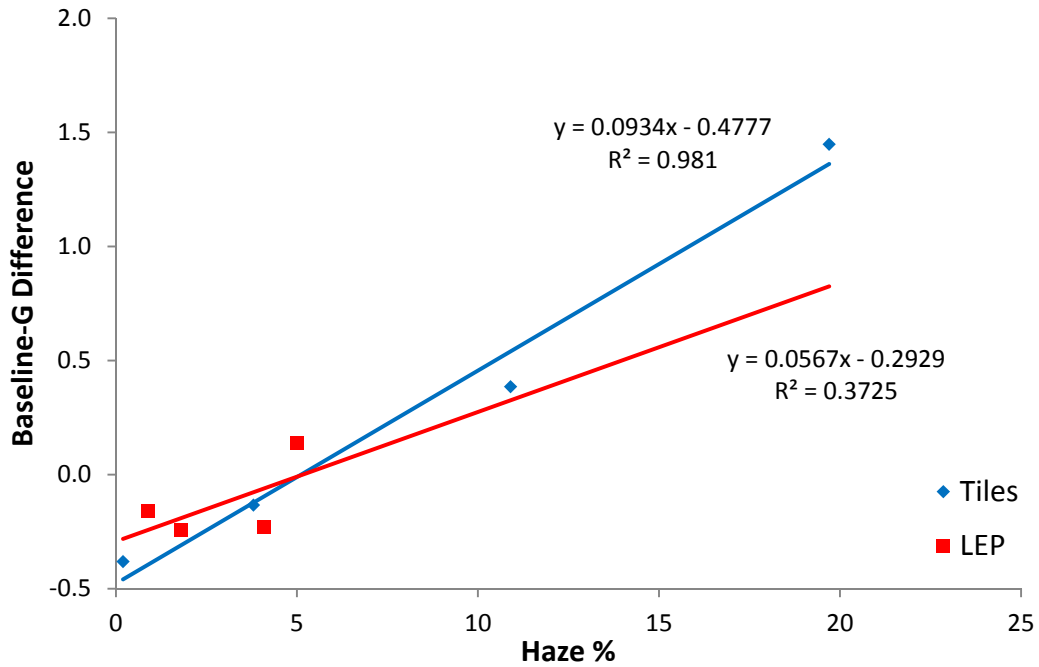


**Figure 12. The difference in AUF between the baseline and OM's in the Glare condition plotted against haze (%) for the haze standards (Tiles) and LEP**

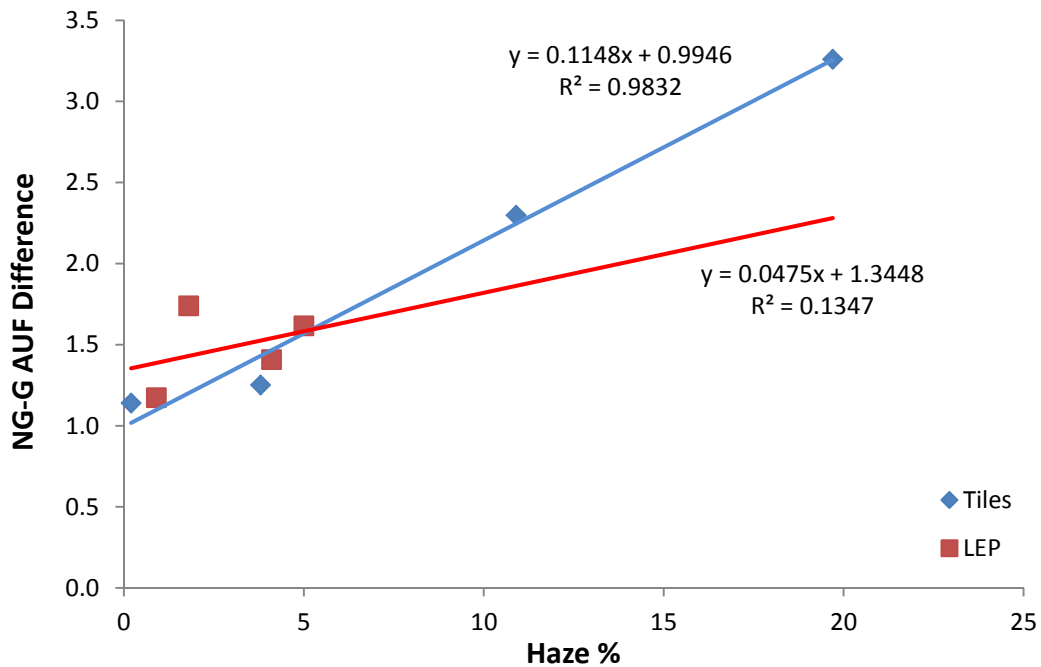


**Figure 13. The differences in AUF between the No Glare and Glare conditions plotted against haze (%) for the haze standards (Tiles) and LEP**

**Table 6. Haze: Slopes and  $R^2$  from the linear regression fits to the baseline AUF difference function and NG-G AUF difference function slope data plotted against percent haze.**

		<b>BASE DIFF NO GLARE</b>	<b>BASE DIFF GLARE</b>	<b>NG-G DIFF</b>
<b>LEP</b>	Slope	0.009	0.057	0.048
	$R^2$	0.004	0.372	0.135
<b>TILES</b>	Slope	-0.021	0.093	0.115
	$R^2$	0.560	0.981	0.983

**Table 7. BTDF: Slopes and  $R^2$  from the linear regression fits to the baseline AUF difference function and NG-G AUF difference function slope data plotted against scatter  $>2^\circ$ ,  $>12^\circ$  and  $>12^\circ$  for LEP and scatter  $>2^\circ$ ,  $>15^\circ$  and  $>8^\circ$  for haze tiles for the three comparisons, respectively. \* Indicates virtual tie with  $R^2$  for same comparison with log (s) in Table 7**

		<b>BASE DIFF NO GLARE</b>	<b>BASE DIFF GLARE</b>	<b>NG-G DIFF</b>
<b>LEP</b>	Slope	1.770	1.984	2.197
	$R^2$	0.067	<b>0.715*</b>	<b>0.452</b>
<b>TILES</b>	Slope	0.035	3.241	0.921
	$R^2$	<b>0.625</b>	<b>0.984</b>	<b>0.994</b>

**Table 8. Log (s): Slopes and  $R^2$  from the linear regression fits to the baseline AUF difference function and NG-G AUF difference function slope data plotted against C-Quant log (s).  
\* Indicates virtual tie with  $R^2$  for same comparison with BTDF in Table 6**

		<b>BASE DIFF NO GLARE</b>	<b>BASE DIFF GLARE</b>	<b>NG-G DIFF</b>
<b>LEP</b>	Slope	-1.625	2.730	1.104
	$R^2$	<b>0.103</b>	<b>0.713*</b>	0.060
<b>TILES</b>	Slope	-0.482	2.287	2.769
	$R^2$	0.454	0.942	0.916

## 4 DISCUSSION

In a previous study Dykes *et al.*[4] reported differences between reflective LEP and haze standards in the amount of acuity decrement from baseline as a function of measured haze when an external glare source was present. For the reflective LEP the level of decrement increased at more than twice the rate as haze increased than it did for the haze standards. A set of LEP that incorporated absorptive technologies gave results nearly identical to those of the haze standards. In addition, for the haze standards, percent haze accounted for nearly 99% of the variance in performance with glare present. The amount of variance accounted for by haze for the reflective LEP was less at 75% and this coupled with the large difference in rate of acuity loss suggested that another factor in addition to haze may be contributing to the rapid acuity decline with glare.

The present study set out to partially replicate the Dykes *et al.*, study using a similar set of haze standards (same type, same manufacturer) but a different set of reflective LEP, an additional measure of spatial vision, and two additional measures of light scatter besides percent haze. The idea of looking at other scatter metrics was to determine if they might better account for the results. The spatial CSF was added to break spatial vision down into individual frequency components that cannot be achieved with letter stimuli, which consist of more than one spatial frequency.

Some results of the present study obtained on the contrast acuity test with the haze standards compare well with the findings of Dykes *et al.*, but others for the LEP do not. Like Dykes *et al.*, we found in the comparisons to baseline, almost no correlation in the No Glare condition between percent haze and decline in acuity as letter contrast decreased for both the LEP and haze samples. When glare was a factor, percent haze was an excellent predictor of the decline in acuity for the haze samples. This correlational finding was true whether the comparison was with the baseline or a more direct analysis within filter comparison between the No Glare and Glare conditions. For the LEP there was almost no association between percent haze and change in acuity for the comparison with baseline in the Glare condition. In contrast, Dykes *et al* found a relatively strong association with the major difference to the haze standards being the rate of acuity decline with measured haze. It is difficult to explain this difference other than that we used a different, and smaller, set of reflective LEP, although our set covered a wider haze range. It is possible that PLT may have contributed to the Dykes finding as three of their seven LEP has PLT in the low-to-mid 40% range and they generated the largest fall-offs in acuity as letter contrast decreased. However, our LEP set had one filter with a PLT in the same range and with higher percent haze than any of their reflective samples; but in terms of acuity performance, this filter gave the best result of our LEP group in the Glare condition.

On the other hand if the direct effect of glare on acuity with LEP was analyzed, then the association with percent haze improved significantly, although this was not to the level reported by Dykes *et al.* What we found is that for the LEP, the total amount of scatter at angles greater than 15° provided the strongest association with acuity performance in glare for both the baseline and direct NG-G comparisons. For the baseline – LEP comparison, scatter >15° accounted for approximately 50% of the variance in performance and for the direct NG-G comparison provided nearly all of the variance (98.6%). Log (s) also had a moderately strong correlation with change in performance in the NG-G comparison, but given the very strong association for scatter >15°, would not likely improve prediction in a multi-predictor model. However, combining log (s) with the BTDF scatter metric may improve prediction for the Baseline-LEP comparison for the Glare condition.

For SCS, the associations of the scatter metrics with changes in the AUF between baseline – LEP and NG-G with the haze standards were strong for the two comparisons for the Glare condition. All of the scatter metrics were strongly associated with changes in AUF with glare with all  $R^2 > 0.91$ . However, total scatter at angles >15° and >12° yielded the highest correlations. In contrast, for the NG-G MAR comparison total scatter >2° worked best. Presently, it is not clear why scatter at more peripheral angles was a better predictor for AUF differences and cumulative scatter at nearly all angles measured worked best for MAR.

Scatter from the BTDF at peripheral angles was also the best predictor of SCS performance change for the two glare comparisons, although log (s) was nearly as good for the Baseline-LEP Glare condition and a two-factor model may improve the correlation. For the Baseline-LEP No Glare condition, none of the scatter metrics showed more than a weak association with performance change. Those associations were stronger for the haze standards but only moderately strong and the best was percent haze.

The ability of scatter metrics derived from the BTDF to best account for changes in CA and SCS, with reflective LEP in the presence of glare, suggests that this measurement should be made as part of the process of optical testing of laser eye protection. Percent haze, the traditional measure, was not particularly effective and for the most part neither was log (s). It seems that for the reflective LEP, scatter at more peripheral angles than those represented in log (s) is an important factor influencing visual performance in glare. However, prior to development of a BTDF requirement for reflective LEP more devices over a wider haze range need to be tested. The present study only assessed four LEP; a minimal number for conclusions to be derived from regression analysis. Also the LEP tested were all dielectric stack technology. Holographic reflective technology should also be evaluated as should LEP with mixtures of absorptive (dyes) and reflective technologies, as well as LEP with different placement of the reflective technology with respect to the substrate. For example, some military LEP consist of two elements, a cap and a base with the dielectric coating sandwiched between them while other LEP have only one element with the dielectric either on the outer or inner surface. There are also differences in components of LEP, such as anti-reflective coatings, that could impact the BTDF.

The objective data collected in this study need to be accompanied by subjective data on observer ratings of scatter/haze and acceptability of the LEP for use in the cockpit. Pilot data on one LEP and a haze standard with relatively high levels of haze, 7.8% and 6.5%, respectively, collected by Gregg Irvin (personal communication, 2015) yielded an interesting result. The LEP reduced acuity and contrast sensitivity less than the haze sample, but, in an outdoor setting, was rated as having lower visibility and higher haze. The differences were attributed to differences in the distribution of scatter in the two OM with the LEP having relatively more scatter at peripheral angles than the haze standard. The distribution of scatter in the LEP used in the present study compared to the haze standards (see Figure 14) indicates a similar difference with relatively more scatter at peripheral angles in the LEP and suggests, for the subjective rating of visibility and perceived haze, a result similar to that obtained by Irvin. At the same time, however, our results (see Figures 9 and 13) indicate that LEP with haze levels  $\leq 5\%$  will yield visual performance equivalent to or worse than the haze standards. Whether or not this will effect subjective ratings needs to be determined with additional LEP, more subjects, and the assessment conducted occurring in better controlled conditions.

Another factor that needs to be considered is what comparison is most relevant to effects on vision under operational conditions. Is it the effect of OM's relative to no OM's (baseline) with glare present that is most important or simply the effect that glare has compared to no glare for a specific OM? An argument can be made that both comparisons are important and, in the present study, both were analyzed. The comparison of performance with LEP versus baseline is important to quantifying the cost of putting on an LEP while the NG-G comparison provides

important information for aircrew on what to expect while wearing LEP in changing glare conditions. For the haze standards, the drop off in performance for either comparison was relatively well accounted for by any one of the scatter metrics. For the LEP, there were some large differences between the comparisons in how well a particular metric predicted the drop in performance with glare. This was particularly true for log (s).

## 5 REFERENCES

1. Thomas, S.R. (1994). "Aircrew laser eye protection: Visual consequences and mission performance," *Aviat., Space, and Environ. Med., Supplement A*, A108- A115.
2. Human Systems Group, United States Air Force. (2005). Performance Specification for the Block 2 Aircrew Laser Eye Protection (ALEP) System; Main body (Unclassified). HGU-APA-01-Block2 ALEP/PS001.
3. Ghani, N., Dykes, J., Garcia, P., Schmeisser, E., Maier, D., and McLin, L.N. (2001). The Effect of Glare on Regan Contrast Letter Acuity Scores Using Dye-Based Laser Eye Protection. AFRL-HE-BR-TR-2001-0094. USAF Research Laboratory, Brooks City-Base TX 78235.
4. Dykes J, Garcia P, Maier D, McLin L, Ghani N, Schmeisser E, Harrington K. (2004). Quantifying the Effects of Haze in Laser Eye Protection on Regan Contrast Letter Acuity. AFRL-HE-BR-TR-2004-0055. USAF Research Laboratory, Brooks City-Base TX 78235.
5. Marasco PE, Task HL. (1999). The effect on vision of light scatter from HMD visors and aircraft windscreens. Proc. SPIE 3689, Helmet- and Head-Mounted Displays IV.
6. ASTM –D1003-13. Standard Test Method for Haze and Luminous Transmittance of Transparent Plastics.
7. Franssen L, Coppens JE, van den Berg, TJTP. (2006) Compensation comparison method for assessment of retinal stray light. *Investigative Ophthalmology and Visual Science*, 47:768-776.
8. IJspeert JK, de Waard PW, van den Berg TJ, de Jong PT. (1990) The intraocular straylight function in 129 healthy volunteers; dependence on angle, age and pigmentation. *Vision Res.* 30:699–707.
9. Regan D, Neima D, (1983) Low-contrast letter charts as a test of visual function. *Ophthalmology*, 90:1192-1200.